Embedded rough surfaces in a 3D constitutive model for concrete

S.C. Hee, A.D. Jefferson & T. Bennett
Cardiff University, Wales, U.K.

ABSTRACT: A two-phase contact model is proposed for the simulation of aggregate interlock behaviour within cracked concrete. The cracked material is decomposed into fine and coarse components, from which the local stress is obtained in a process similar to that used in the theory of mixtures. The model is validated against experimental data from some shear-normal tests. Despite some discrepancies between measured and predicted stress values, the numerical predictions have similar trends to those of the experimental results.

Keywords: aggregate interlock, contact, damage, plasticity, concrete

1 INTRODUCTION

The formation of micro-cracks is largely responsible for the highly non-linear stress-strain behaviour of concrete, with increasing micro-cracking causing progressive weakening of the material and the apparent overall degradation of elastic properties and the formation of inelastic strains (Imran & Antazopoulou 1996). It has been widely accepted that continuum damage mechanics provides a natural framework for simulating the deterioration of material stiffness as well as the loss of material strength, but it has also been acknowledged that this theory is not able to represent the permanent straining that results from the micro-cracking process but that this latter phenomenon can be properly simulated using the theory of plasticity.

Over the past few decades, considerable effort has been devoted to developing numerical models for the description of this complex behaviour of concrete. Both plasticity models (Este & Willam 1994; Imran & Pantazopoulou 1996; Grassl et al. 2002) and damage models (Ortiz 1985; Oliver et al. 1990; Brencich & Gambarotta 2001; Luccioni & Oller 2003) have been developed to simulate the non-linear behaviour of concrete. Gradually more comprehensive concrete models have been produced as the understanding of the behaviour of material has developed. Many researchers have proposed constitutive models that employ both damage and plasticity formulation to capture the responses of concrete under tension and compression (Lubliner 1989; Luccioni et al. 1996; Lee & Fenves 1998; Meshke et al. 1998, Hansen et al. 2001).

Experimental evidence on shear transfer across crack faces has intrigued many researchers and led them to develop numerical models that are capable of simulating the mechanisms governing the stress transfer. Many have looked into ways of predicting the full behaviour of a crack interface subjected to both normal and shear stresses (Bažant et al. 1980; Walraven 1981; Li et al. 1989). In an assessment of these models by Feenstra et al. 1991, the contact density model of Li et al. was found to provide the numerical predictions with the greatest accuracy when measured against observed experimental behaviour. Wu and his colleagues (Wu et at. 1994) have proposed a plastic-fracture stress transfer model to simulate the behaviour of concrete discontinuities with contact surface degradation, dilatancy, and material non-linearity. An explicit relationship between stress increments and relative discontinuity displacements at all possible interfaces across the crack was developed to provide a more realistic representation of concrete discontinuities.

A number of experimental studies have been published, which have been aimed at understanding

the behaviour of cracks under combined normal and shear loading (Hassanzadeh 1991; Nooru-Mohamed 1992; Gálvez et al. 1998; Cendón et al. 2000), whose data have been used to verify normal/shear cracking of concrete models. A proper concrete crack model should be capable of simulating both monotonic and cyclic behaviour of the cracked material (Olofsson 1995; Carol et al. 1997; Bažant et al. 2000). The aforementioned crack plane models employ a plasticity approach to capture some of the behaviour of cracks under combined normal and shear loading.

Experimental evidence has shown that there is a possibility for an open crack to regain contact in shear, resulting in a distribution of the normal and shear stresses across the crack interface with a residual positive opening displacement (Walraven & Reinhardt 1981).

Jefferson (2003a, b) has utilised a combined plastic-damage-contact theory in a new constitutive model for concrete, which is able to simulate with reasonable accuracy crack closure, shear contact and aggregate interlock behaviour as well as the general non-linear behaviour of concrete in compression up to moderate degrees of confinement. The model uses planes of degradation that can undergo damage and separation but that can regain contact according to a contact law. The model, known as Craft, has been developed within a thermodynamically consistent framework and has been implemented in the finite element program LUSAS.

The contact model within Craft was a simplified version of a more detailed crack plane model Jefferson (2002). It is the further development of the embedded contact component within the Craft model that is the focus of the present work. The formulation of the new two-phase contact surface was derived using experimental data from Walraven and Reinhardt (1981) and Hassanzadeh (1991).

2 CRACK SURFACE CHARACTERISATION

Experimental evidence has shown that the overall shear strength of a material is affected by the type, shape and size of aggregate particles. In normal strength concretes, both fine and coarse aggregate particles are evenly distributed within the mortar matrix. Large mismatches between the elastic moduli of aggregate and mortar matrix prevents cracks from penetrating into the aggregate particles. Crack paths tend to move towards the interface between aggregate and mortar, a region which is normally regarded as the weakest link in concrete (Karihaloo 1995). Figure 1 illustrates the path of a typical crack within a normal strength concrete matrix that comprises both coarse and fine aggregate particles. Paulay and Loeber (1974) undertook experiments to investigate the behaviour of such cracks in shear and, as may be seen from Figure 2, their results show that with increasing shear movement, for an open crack, the stiffness increases significantly at a certain shear displacement. Similar behaviour is also seen in other such data (e.g. Walraven & Reinhardt 1981). In Jefferson (2002a) this stiffness increase point was taken as the first contact point and used to define the contact 'Interlock' surface. However, this ignores the fact that there are significant shear stresses before this point is reached. In order to better simulate the observed behaviour, a two-phase contact model is explored in which, tentatively, the two components are associated with the mortar and coarse aggregate components.

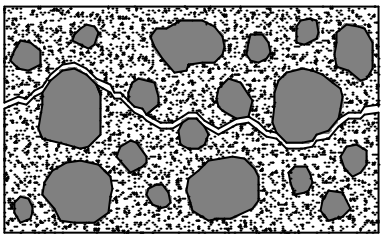

Figure 1. Crack profile

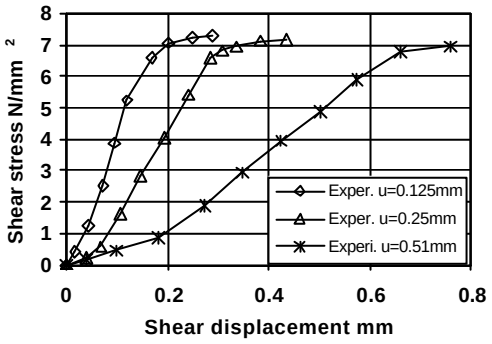

Figure 2. Shear stress-displacements from Paulay and Loeber.

3 NUMERICAL MODEL

As mentioned in previous section, the present model is a development of the Craft model that employs a combination of plasticity, damage and contact theories. In the model the local crack-plane strains are related to the relative displacements on the crack plane via a characteristic length parameter.

3.1 Damage-contact model

The damage-contact model employed in Craft is a simplified version of the crack plane model originally proposed by the same author (Jefferson 2002). A relationship between the local stress and effective strain is derived, in which the local stress on each crack plane is taken as the sum of the contribution of stresses from the undamaged and contact components

$$\boldsymbol{s} = \boldsymbol{D}_L(h_c\boldsymbol{e} + h_f\,\boldsymbol{g}) = \boldsymbol{D}_L(h_c\boldsymbol{I} + h_f\boldsymbol{F}_d)\boldsymbol{e} \qquad (1)$$

where h_c and h_f denote the undamaged and contact component respectively. $\boldsymbol{D}_L$ is the local elastic constitutive matrix, $\boldsymbol{I}$ is the identity matrix and F_d is a transformation matrix. The compressive contact strain is denoted by the vector $\boldsymbol{g}$, which has a magnitude g representing the nearest distance to the interlock surface.

Figure 3 shows a schematic diagram of the contact model. In the open state, the stress in the contact component is assumed to be zero. In the interlock state, the embedment $\boldsymbol{g}$ is taken as the distance to the interlock contact surface. In the closed state, $\boldsymbol{g}$ is equal to the local strain vector as the contact point coincides with the origin of the local strain space. The following expressions are the interlock and closed functions, which are used to define the state of contact on a crack plane.

$$f_{int}(\boldsymbol{e}) = m_g\, e_r - \sqrt{e_s^{\,2} + e_t^{\,2}} \qquad (2)$$

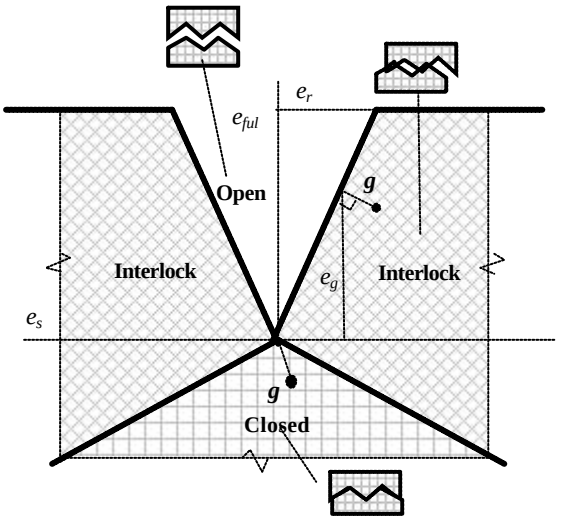

Figure 3. Contact states and embedment.

$$f_{cl}(\boldsymbol{e}) = e_r + m_g\sqrt{e_s^{\,2} + e_t^{\,2}} \qquad (3)$$

If $f_{cl}(\boldsymbol{e}) = 0$ State = Closed
If $f_{cl}(\boldsymbol{e}) > 0$ and $f_{int}(\boldsymbol{e}) < 0$ and $e_r < e_{ful}$ State = Interlock
If $f_{int}(\boldsymbol{e}) = 0$ or $e_r = e_{ful}$ State = Open

m_g is the gradient of the interlock function, and e_{ful} denotes the local opening strain beyond which no further contact can be gained in shear. e_{ful} is obtained by multiplying the strain at the end of the softening curve e_0 with a multiplier constant m_{ful}, for the contact function.

The value of m_g is obtained from experimental data in which shear loading is applied to an open crack. With reference to the test conducted by Walraven and Reinhardt (1981), it is found to be reasonable to have m_g in the range 0.3-0.6 for normal strength concrete. For concrete that comprises relatively large coarse aggregate particles (i.e. 20-30 mm), a value of m_{ful} in the range 10-20 is appropriate, whereas for relatively small coarse aggregates (i.e. 5-8 mm), a lower value in the range 3-5 is appropriate (Jefferson 2003a).

A plane of degradation (POD) is formed once the major principal stress exceeds the fracture strength. For the formation of successive crack planes, a tolerance angle a_p is introduced to ensure that new PODs are not too close to existing planes. Figure 4 shows a schematic diagram of the damage surface used in the model, which was similar in shape to that of Kroplin and Weihe (1997). z is the damage strain parameter and r_z is the strain equivalent of the relative shear stress intercept.

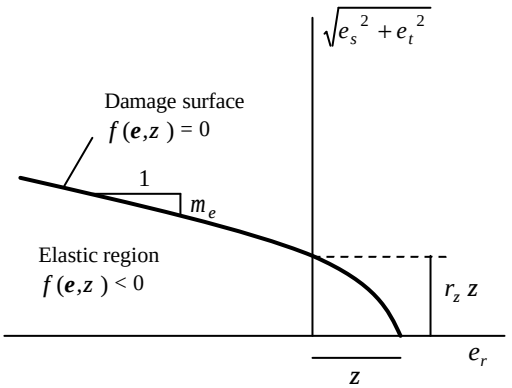

Figure 4. Damage surface in local strain space.

Considering Equation 1, the relationship between the local stress and effective strain can also be written as

$$\boldsymbol{s} = \boldsymbol{D}_L(h_c\boldsymbol{I} + h_f\boldsymbol{F}_d)\boldsymbol{e} = \boldsymbol{D}_L\boldsymbol{M}_x\boldsymbol{e} \quad (4)$$

where $\boldsymbol{M}_x$ is the contact matrix. The inelastic component of $\boldsymbol{e}$, also known as the added fracture local strain vector, is denoted by $\boldsymbol{e}_f$, as follows

$$\boldsymbol{e}_f = \boldsymbol{e} - \boldsymbol{C}_L\boldsymbol{s} \quad (5)$$

where $\boldsymbol{C}_L$ is the inverse of the local elastic constitutive matrix. Using Equation 4 in 5 gives an expression that relates the added fracture local strain to the local stress

$$\boldsymbol{e}_f = (\boldsymbol{M}_x^{-1} - \boldsymbol{I})\boldsymbol{C}_L\boldsymbol{s} = \boldsymbol{C}_{lsf}\boldsymbol{s} \quad (6)$$

where $\boldsymbol{C}_{lsf}$ is the local compliance matrix.

3.2 Plasticity Model

In simulating the compressive behaviour of the material, the model employs a triaxial yield surface and plastic potential based upon the compressive meridians after Lubliner et al. (1989). The surface, as illustrated in Figure 5, is enhanced by introducing a smoothing function developed by Willam and Warnke (1975).

The model employs a frictional work hardening and softening law to account for pre and post peak nonlinear behaviour. It is assumed that the amount of work to achieve peak stress increases with the mean stress, in which a parameter is introduced that has the same function as the ductility parameter of Este and Willam (1994). A dilatancy parameter is included to allow for the plastic flows to be associated or non-associated. Details of the plasticity model and its implementation are described elsewhere (Jefferson 2003a).

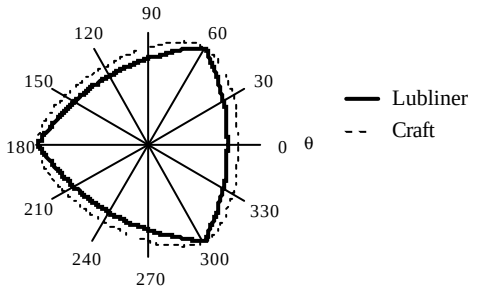

Figure 5. Yield surface in octahedral plane.

3.3 Two Component Contact Model

A new two-phase contact model is proposed in which two contact surfaces are introduced, each of which captures the contact states of the damaged component on a crack plane. Considering Equation 1 from the previous section, a new parameter a_c, i.e. the proportion of coarse particles in a representative volume of the fully debonded material, is introduced in the current model to enhance the damage-contact component of the constitutive model. The relationship between the local stress and effective strain is now written as

$$\boldsymbol{s} = \boldsymbol{D}_L[h_c\boldsymbol{I} + a_c h_{fc}\boldsymbol{F}_{dc} + (1-a_c)h_{ff}\boldsymbol{F}_{df}]\boldsymbol{e} \quad (7)$$

where both h_{fc} and h_{ff} govern the fully debonded component, with the subscripts *fc* and *ff* denoting the fraction of coarse and fine particles, respectively, in a representative volume of the damaged material.

The material parameters that define the contact surface, i.e. the slope of interlock function m_g, and multiplier constants m_{hi} and m_{ful}, are now required for both the coarse and fine components. m_{hi} is the multiplier of the strain that governs the point at which contact starts to reduce. As discussed in Section 2, for large opening displacements, the coarse component is assumed to control the overall stress due to the aggregate interlock behaviour, whereas at small opening displacements the fine component is also significant. Using the experimental data of Walraven and Reinhardt (1981), as shown in Figure 6, the m_g values were determined by treating the first half of the non-linear curve as being influenced more by the fine component, and the second half by the coarse component. In the current model, the m_g value for the fine component is taken as 0.2 and for the coarse component as 0.4.

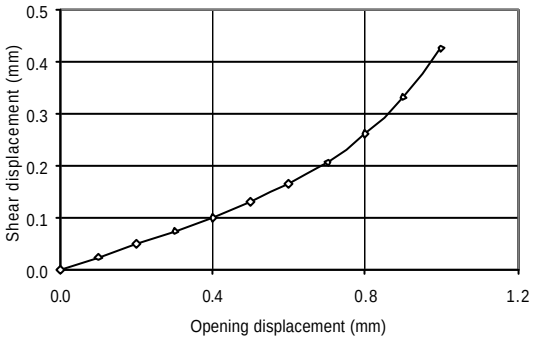

Figure 6. Normal-shear contact relationship (Walraven and Reinhardt 1981).

A number of images captured using a Scanning Electron Microscope (SEM) at the meso-level have been gathered from which an average measurement of the crack surface roughness has been obtained (Ollivier 1985; van Mier 1997). The procedure for deriving the contact parameters for the two-phase model, with reference to Figure 7, is as follows; a mean reference crack line is drawn parallel to the direction of crack propagation, which intersects aggregate particles whose perimeters form part of the crack faces. By taking several sampling points along the crack, the distances between the free surface and reference line are measured, i.e. c_i and f_j for the coarse and fine components respectively, where i and j denote the number of sampling point for the coarse and fine particles respectively along the crack reference line. Thereafter, the average values of the surface roughness m_{ful} for each of the two components are obtained. These allow for an estimate of the ratio between the m_{ful} values of both fine and coarse components, which lies in the range 0.3-0.6. In addition, the proportion of the crack length over which the surface roughness of coarse aggregate applies is determined. This provides an estimate of the percentage of coarse particles present within the concrete matrix ($a_c=l_c/L$). Having examined a number of SEM images, it was found that a_c falls in the range 0.3-0.4.

4 NUMERICAL EXAMPLES

In this section, the results obtained from numerical simulations are compared with those from experimental studies. Experimental tests conducted by Walraven and Reinhardt (1981) and Hassanzadeh (1991), which involve the application of normal and shear loadings on concrete specimens, are chosen for comparisons and to validate the proposed model. Table 1 gives the material parameters used in the analyses.

Table 1. Material properties used for analyses.

Material Parameters	Ex. 1	Ex. 2
Young's modulus E (N/mm^2)	30000	50000
Poisson's ratio u	0.15	0.15
Comp. strength f_c (N/mm^2)	29.5	40
Tensile strength f_t (N/mm^2)	2.5	3
Strain at peak uniaxial stress e_c	0.0022	0.0023
Strain at end of softening curve e_0	0.0026	0.0
Fracture energy G_F (N/mm)	0.0	0.1
m_g (coarse / fine)	0.4/0.2	0.4/0.2
m_{hi} (coarse / fine)	3.0/1.5	0.4/0.2
m_{ful} (coarse / fine)	13.5/9.0	2.0/1.0
a_c	0.3	0.3

4.1 Walraven and Reinhardt's Tension-Shear Tests

This example involves a numerical simulations based on the normal-shear tests undertaken by Walraven and Reinhardt (1981). Figure 8 shows an illustration of the test specimens, which had a shear plane of 300 × 120mm^2 and were tested in a stiff testing frame with external restraints bars to control the crack opening displacement. All specimens were initially loaded in tension to a set initial crack opening displacement before being loaded in shear. The tests were denoted by the code *a*/*b*/*c* where '*a*' is the the concrete mix number, '*b*' the nominal opening and '*c*' the normal stress at an arbitrary crack width of 0.6mm. The tests were conducted with three different nominal values of opening displacement, i.e. 0.0, 0.2 and 0.4mm, and for each of the three nominal values, two tests were conducted.

Figures 9 and 10 show the variation of normal and shear stress with the corresponding displacement, respectively. At the initial stage of loading, the model predicts results that are within the bounds of the two experimental curves, after which it over-predicts the stress-displacement response. However, at the final stage of loading, the response gradually decreases and moves back to within the boundaries.

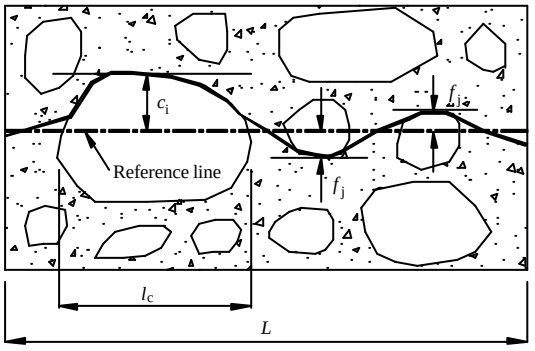

Figure 7. Derivation of contact parameters.

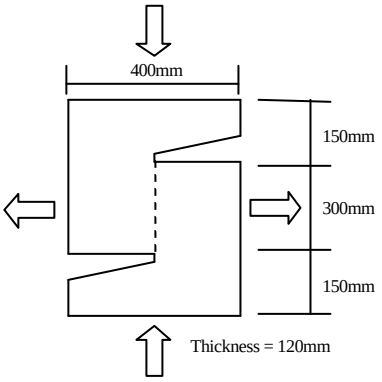

Figure 8. Walraven & Reinhardt's test specimen.

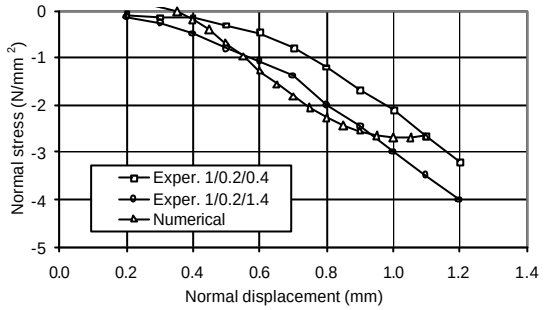

Figure 9. Normal stress-displacement relationship.

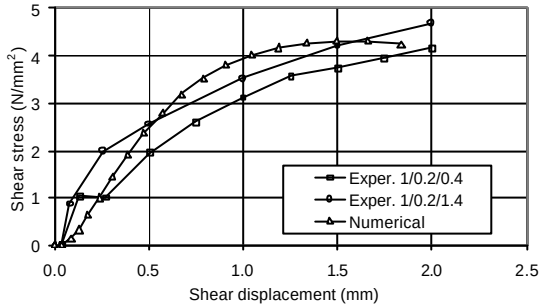

Figure 10. Shear stress-displacement relationship.

4.2 Hassanzadeh's Tension-Shear Test

The example presented here is an analysis based on an experimental study undertaken by Hassanzadeh (1991). In the tests, feedback loops where used to link shear and normal displacements to the associated loads. The test specimen is illustrated in Figure 11 and has an effective cross-section at the notch level of 40 × 40mm^2. The finite element mesh comprises of 8-noded quadratic elements. The testing procedure involved firstly applying tension to the point of first fracture (at the top of the softening curve) and then applying displacements according to $u = (\tan\alpha)v$. The tests considered here are those with $\alpha = 45°$ and $\alpha = 60°$.

Figure 12 shows the numerical crack plots at the final step of the analyses. Figures 13-16 give the stress-displacement responses and provide comparisons of the numerical predictions with that of experimental results. As can be seen in Figures 13 and 14, the trends in the numerical results are similar to those of the experimental.

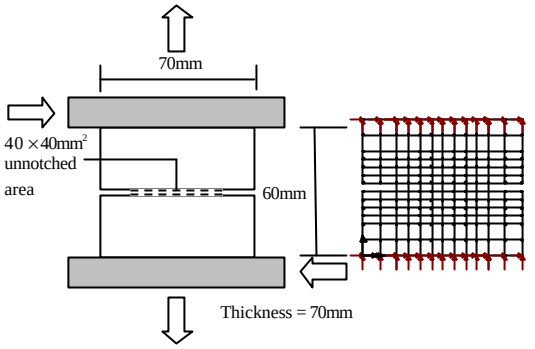

Figure 11. Hassanzadeh's test specimen.

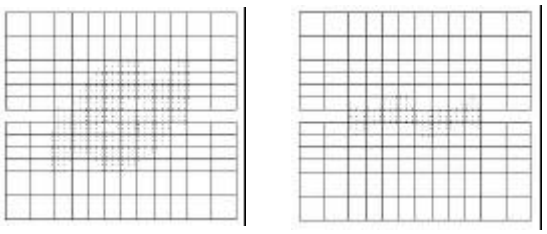

Figure 12. Crack plots for (a) $\alpha = 45°$, and (b) $\alpha = 60°$.

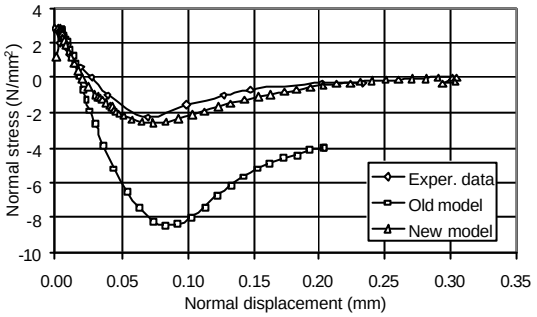

Figure 13. Normal stress-displacement relationship ($\alpha = 45°$).

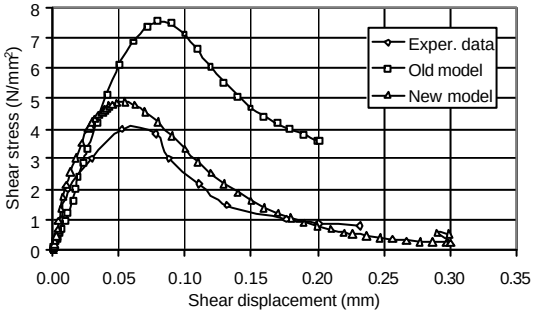

Figure 14. Shear stress-displacement relationship ($\alpha = 45°$).

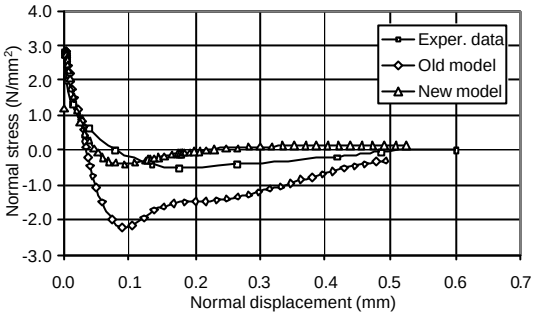

Figure 15. Normal stress-displacement relationship ($\alpha = 60°$).

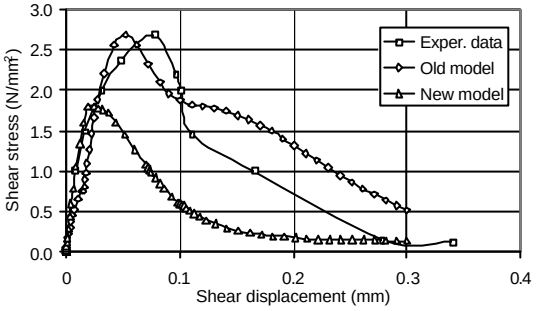

Figure 16. Shear stress-displacement relationship ($\alpha = 60°$).

5 DISCUSSION AND CLOSING REMARKS

The proposed two-phase contact model is able to simulate the behaviour of aggregate interlock in cracked concrete. Although perfect agreement with experimental results has yet to be achieved, the model does predict similar trends to those observed in experiments. It should be noted that the results obtained in both numerical examples were based on a different set of constants used in the contact component. Therefore, further refinement in the contact model is required in order to expand its applicability and to achieve good matches to a wide range of experimental data.

REFERENCES

Bažant, Z. & Gambarova, P. 1980. Rough cracks in reinforced concrete. *J. Struct. Div. ASCE*, 106(4), 819-842.

Bažant, Z.P., Caner, F.C., Carol, I., Adley, M.D. & Akers, S.A. 2000. Micro-plane model M4 for concrete. I Formulation with work conjugate deviatoric stress. *J. Engng. Mech. ASCE*, 126(9), 944-953.

Brencich, A. & Gambarotta, L. 2001. Isotropic damage model with different tensile-compressive response for brittle materials, *Int. J. Solids Struct*., 38, 5865-5892.

Carol, I., Prat, P.C. & López, C.M. 1997. Normal-shear cracking model: Application to discrete crack analysis. *J. Engng. Mech. ASCE*, 123(8), 765-773.

Cendón, D.A., Galvez, M., Elices, M. & Planas, J. 2000. Modelling the fracture of concrete under mixed loading. *Int. J. Fract.*, 103, 293-310.

Este, G. & Willam, K. 1994. Fracture energy formulation for inelastic behavior of plain concrete. *J. Engng. Mech. ASCE*, 120(9), 1983-2011.

Feenstra, P.H., de Borst, R. & Rots, J.G. 1991. Numerical study on crack dilatancy. II. Applications. *J. Engng. Mech. ASCE*, 177(4), 754-769.

Gálvez, J.C., Elices, M., Guinea, G.V. & Planas, J. 1998. Mixed mode fracture of concrete under proportional and nonproportional loading, *Int. J. Fract.*, 94, 267-284.

Grassl, P., Lundgren, K. & Gylltoft, K., 2002. Concrete in compression: a plasticity theory with a novel hardening law. *Int. J. Solids Struct.*, 39, 5205-5223.

Hansen, E., Willam, K. & Carol, I. 2001. A two-surface anisotropic damage/plasticity model for plain concrete, In de Borst, R., Mazars, J., Pijaudier-Cabot, G. & van-Mier, J.G.M. (eds.), *Proc. of 4th Int. Conf. Fracture Mechanics of Concrete Materials*, Framcos-4, Paris.

Hassanzadeh, M. 1991. Behaviour of fracture process zones in concrete influenced by simultaneously applied normal and shear displacements. *PhD Thesis*, Lund Institute of Technology, Sweden.

Imran, I. & Pantazopoulou, S. 1996. Experimental study of plain concrete under triaxial stress. *ACI Mater. J.*, 93(6), 589-601.

Jefferson, A.D. 2002. Constitutive modelling of aggregate interlock in concrete. *Int. J. Numer. Anal. Meth. Geomech.*, 26(5), 515-535.

Jefferson, A.D. 2003a. Craft, a plastic-damage-contact model for concrete. I. Model theory and thermodynamic considerations. *Int. J. Solids Struct.*, 40(22), 5973-5999.

Jefferson, A.D. 2003b. Craft, a plastic-damage-contact model for concrete. II. Model implementation with implicit return mapping algorithm and consistent tangent matrix. *Int. J. Solids Struct.*, 40(22), 6001-6002.

Karihaloo, B.L. 1995. Fracture mechanics and structural concrete. New York: Longman.

Kroplin, B. & Weihe, S. 1997. Aspects of fracture induced anisotropy. *Proc. of 5th International conference on computational plasticity (COMPLAS5)*, Barcelona, 255-279.

Lee, J. & Fenves, G.L. 1998. Plastic-damage model for cyclic loading of concrete structures. *J. Engng. Mech. ASCE*, 124, 892-900.

Li, B., Maekawa, K. & Okamura, H. 1989. Contact density model for stress transfer across cracks in concrete. *J. Faculty of Engineering*, 40(1), 9-52.

Lubliner, J., Oliver, J., Oller, S. & Onate, E. 1989. A plastic-damage model for concrete. *Int. J. Solids Struct.*, 25(3), 299-326.

Luccioni, B., Oller, S. & Danesi R. 1996. Coupled plastic-damaged model. *Comput. Meth. Appl. Mech. Engng.*, 129, 81-89.

Luccioni, B. & Oller, S. 2003. A directional damage model. *Comput. Methods Appl. Mech. Engng.*, 192(9-10), 1119-1145.

Meshke, G., Lackner, R. & Mang, H.A. 1998. An anisotropc elastoplastic-damage model for plain concrete. *Int. J. Numer. Meth. Engng.*, 42, 703-727.

Nooru-Mohamed, M.B. 1992. Mixed-mode fracture of concrete: an experimental approach. *PhD. Thesis*, Delft University of Technology, Netherlands.

Oliver, J., Cervera, M., Oller, S. & Lubliner, J. 1990. Isotropic damage models and smeared crack analysis of concrete. *Computer Aided Analysis and Design of Concrete Structures*, Pinebridge Press, Swansea, England, 945-957.

Ollivier, J.P. 1985. A non destructive procedure to observe the microcracks of concrete by scanning electron-microscopy. *Cement and Concrete Research*, 15(6), 1055-1060.

Ortiz, M. 1985. A constitutive theory for the inelastic behaviour of concrete. *Mech. Mater.*, 4, 67-93.

Paulay, T. & Loeber P.J. 1974. Shear transfer by aggregate interlock. In *Shear in reinforced concrete*, Publication SP-42, American Concrete Institute, 1-15.

van Mier, J.G.M. 1997. Fracture Process of Concrete. CRC Press, Florida.

Walraven, J. 1981. Fundamental analysis of aggregate interlock. *J. Struct. Div. ASCE*, 107(11), 2245-2270.

Walraven, J.C. & Reinhardt, H.W. 1981. Theory and experiments on the mechanical behaviour of cracks in plain and reinforced concrete subjected to shear loading. *Heron*, 26(1A), Delft, Netherlands.

Willam, K. & Warnke, E. 1975. Constitutive models for triaxial behaviour of concrete. *Proc. Int. Assoc. Bridge Struct. Engng.*, Report 19, Zurich, Switzerland. 1-30.

Wu, Z., Farahat, A.M. & Tanabe, T. 1994. Plastic-fracture stress transfer model for concrete discontinuities. *ACI Mater. J.*, 91(5), 502-508.